LOXL1 exerts oncogenesis and stimulates angiogenesis through the LOXL1-FBLN5/αvβ3 integrin/FAK-MAPK axis in ICC

Ruiyan Yuan,[1,5] Yang Li,[1,5] Bo Yang,[3,5] Zhaohui Jin,[1] Jiacheng Xu,[4] Ziyu Shao,[1] Huijie Miao,[1] Tai Ren,[1] Yang Yang,[1] Guoqiang Li,[1] Xiaoling Song,[1] Yunping Hu,[1] Xu'an Wang,[2] Ying Huang,[1] and Yingbin Liu[2]

[1]State Key Laboratory of Oncogenes and Related Genes, Department of General Surgery, Shanghai Key Laboratory of Biliary Tract Disease Research, Xinhua Hospital Affiliated to Shanghai Jiao Tong University School of Medicine, Shanghai 200092, China; [2]Department of Biliary-Pancreatic Surgery, Renji Hospital Affiliated to Shanghai Jiao Tong University School of Medicine, Shanghai 200120, China; [3]Key Laboratory of Diagnosis and Treatment of Severe Hepato-Pancreatic Diseases of Zhejiang Province, Department of Surgery, First Affiliated Hospital of Wenzhou Medical University, Baixiang Road, Wenzhou 325000, China; [4]Endoscopy Center and Endoscopy Research Institute, Zhongshan Hospital, Fudan University, No. 180 Fenglin Road, Shanghai 200032, China

Aberrant expression of lysyl oxidase-like 1 (LOXL1) reportedly leads to fibrous diseases. Recent studies have revealed its role in cancers. In this study, we observed an elevated level of LOXL1 in the tissues and sera of patients with intrahepatic cholangiocarcinoma (ICC) compared with levels in nontumor tissues and sera of unaffected individuals. Overexpression of LOXL1 in RBE and 9810 cell lines promoted cell proliferation, colony formation, and metastasis in vivo and in vitro and induced angiogenesis. In contrast, depletion of LOXL1 showed the opposite effects. We further showed that LOXL1 interacted with fibulin 5 (FBLN5), which regulates angiogenesis, through binding to the αvβ3 integrin in an arginine-glycine-aspartic (Arg-Gly-Asp) domain-dependent mechanism and enhanced the focal adhesion kinase (FAK)-mitogen-activated protein kinase (MAPK) signaling pathway inside vascular endothelial cells. Our findings shed light on the molecular mechanism underlying LOXL1 regulation of angiogenesis in ICC development and indicate that the LOXL1-FBLN5/αvβ3 integrin/FAK-MAPK axis might be the critical pathological link leading to angiogenesis in ICC.

INTRODUCTION

Cholangiocarcinoma (CCA) or bile duct cancer is the most common biliary tract cancer and the second-most common primary liver malignancy, accounting for approximately 10%–15% of all primary liver cancers.[1] More specifically, CCA is classified into three subtypes according to its anatomic origin within the biliary tree: intrahepatic, perihilar, and distal CCA. Although intrahepatic CCA (ICC) is more common in Asia, its incidence has increased significantly in Europe and North America in recent decades. Preclinical studies have indicated that inflammation, cholestasis, and some metabolic diseases are the major factors involved in the carcinogenesis of ICC.[2]

Owing to the nonspecific symptoms and highly aggressive nature of ICC, most patients are diagnosed at an advanced stage with a median survival time of less than 2 years,[3] and recurrence after surgery is also common. An in-depth understanding of the molecular biology of this tumor will provide more choices of diagnosis, so as to adopt more effective nonsurgical measures to treat affected patients.

Fibrosis and angiogenesis are known to play important roles in the process of cholangiocarcinogenesis and the deep invasion of the tumor into the liver. Anatomically, the intrahepatic bile ducts are adjacent to liver sinusoidal endothelial cells (LSECs) and the liver parenchyma. LSECs are essential for the formation of intrahepatic capillaries with special structures connecting hepatic cells and inner blood plasma. This anatomic relationship implies that the biological behavior of ICC might be related to its anatomical location.

Lysyl oxidase-like 1 (LOXL1), a key enzyme in elastic fiber synthesis and homeostasis, is a member of the LOX family, all members of which are copper-dependent amine oxidases, including the five paralogs: LOX, LOXL1, LOXL2, LOXL3, and LOXL4. These copper-dependent amine oxidases contain a highly conserved C-terminal domain, sharing a similar catalytic activity, and can regulate the tensile strength and structural integrity of many tissues.[4,5] The LOX

family plays an important role in the construction of the tumor microenvironment in solid tumors by covalently crosslinking collagens and elastin in the extracellular matrix (ECM).[6,7]

Previous studies on LOXL1 have focused extensively on its role in exfoliation and pseudoexfoliation syndromes, despite its involvement in malignancy progression. Guojun Wu's[8] team found that epigenetic silencing of LOXL1 and LOXL4 could inhibit the Ras/extracellular signal-regulated kinase (Erk) signaling pathway in human bladder cancer. In our study, we discovered the role of LOXL1 in promoting proliferation, metastasis, and angiogenesis in ICC. Furthermore, our coimmunoprecipation (coIP) assay identified fibulin 5 (FBLN5) as a synergistic factor of LOXL1 in vascular formation.

FBLN5 was identified by two independent groups in 1999.[9,10] It is a secreted ECM protein with six calcium-binding (CB)-epidermal growth factor (EGF) motif repeats and a globular C-terminal domain typical of other FBLNs,[11] including an evolutionarily conserved arginine-glycine-aspartic (Arg-Gly-Asp [RGD]) motif, known to mediate the assembly of elastic fibers, angiogenesis, and tumorigenesis.[12–14] In addition, further studies have shown that the N terminus of FBLN5 can specifically bind to the αvβ3, αvβ5, and α9β1 integrins, known to be expressed by vascular endothelial cells (VECs),[14] and this ability to bind to integrins depends on its RGD sequence.

In this study, we tested the serum levels of LOXL1 in patients with ICC and normal volunteers and found that the levels of LOXL1 in patients with ICC were higher than those in normal people. Moreover, the expression of LOXL1 in tumor tissues of ICC was also significantly higher than that in adjacent tissues. We further showed that LOXL1 could promote the proliferation and metastasis of ICC tumor cells by regulating epithelial-mesenchymal transition (EMT) and the mitogen-activated protein kinase (MAPK) pathway and stimulate angiogenesis by cooperation with FBLN5 via the interactions between the RGD domain in FBLN5 and the αvβ3 integrin. These findings might be pivotal in understanding the progression and metastasis of ICC tumors, and the discovered signal axis (LOXL1-FBLN5/αvβ3 integrin/focal adhesion kinase [FAK]-MAPK) could potentially serve as a new therapeutic target for ICC antiangiogenetic treatments.

RESULTS

LOXL1 was upregulated and correlated with poor prognosis in patients with ICC

To explore the function of the LOX family in ICC, we compared the relative mRNA levels of the five LOX family members in RBE and 9810 cells. Only the mRNA level of LOXL1 was relatively high in both cell lines (Figure 1A). As an essential part of the extracellular components of the human body, blood is considered critical in detecting local and overall pathological changes. To determine the serum levels of LOXL1 in patients, we collected the same volume of venous blood samples from five normal volunteers and five ICC patients and then concentrated the upper blood serum for further western blot analysis. Our results indicated that secreted LOXL1 was at low levels in all five normal blood samples (Figure 1B). We further evaluated the

protein levels of LOXL1 in 57 pairs of ICC tumor tissues and their adjacent normal counterparts through immunohistochemistry (IHC). We found that the levels of LOXL1 in ICC tumor tissues were higher than those in the adjacent normal tissues (Figures 1C−1E). Moreover, we detected the protein expression of LOXL1 in 12 pairs of tumor tissues and tumor adjacent tissues. The upregulation of LOXL1 in tumor tissues (p < 0.01) exhibited the same trend as that observed in blood serum (Figures 1F and 1G). The results from the clinical specimens were also consistent with the qPCR results from the ICC cell lines. To determine the relationship of the levels of LOXL1 in ICC with clinicopathological parameters, we conducted a detailed analysis of the 57 ICC cases (Table 1). Our results demonstrated that the expression of LOXL1 was positively correlated with the clinical stage of ICC (Figure 1H), microvascular invasion, lymph node metastasis, and liver metastasis. Patients with ICC, with higher levels of LOXL1, were also observed to have a worse overall survival (Figure 1I; p < 0.001). Taken together, a high level of LOXL1 expression might be critical in the progression, microvascular invasion, and metastasis of ICC, and LOXL1 might have the potential to serve as a prognosis-related marker in assessing patients with ICC.

Knockdown of LOXL1 in ICC cells attenuated their proliferation and migration in vitro

To evaluate the function of LOXL1 in the progression of ICC, we knocked down LOXL1 in 9810 and RBE cell lines using small interfering RNA (siRNA). The knockdown efficiency was assessed by both qRT-PCR and western blotting (Figures 2A and 2B). LOXL1 was downregulated in both RBE and 9810 cells as expected. Cell Counting Kit-8 (CCK8) and colony-formation assays were performed to test the changes in cell biological behavior. Upon LOXL1 knockdown, cell proliferation was significantly inhibited compared with that of the negative control (NC) group (Figure 2C). Moreover, there were fewer cell clones in the LOXL1 knockdown group after 14 days of culture (Figure 2D), indicating that downregulation of LOXL1 dramatically reduced the proliferative potential of the tumor cells. Consistently, Transwell assays also showed that fewer cells could pass through the chamber membrane in the knockdown group, which means that the capacity for cell migration was impaired as well after downregulation of LOXL1 in the 9810 and RBE cells (Figure 2E).

Next, we tested the phosphorylation levels of protein kinase B (PKB; also known as pAKT) and pErk1/2, two factors known to be important in cell survival and the growth-associated signaling pathway. pAKT and pErk1/2 were decreased in the LOXL1 knockdown group (Figure S1), implying that LOXL1 could regulate the proliferation and migration ability of ICC cells by affecting pAKT and pErk. These data indicated that LOXL1 indeed played a role in promoting ICC, and following inhibition of its expression, its tumor-promoting function could be reversed in vitro.

LOXL1 promoted ICC tumor growth and angiogenesis both in vitro and in vivo

To further investigate the molecular mechanism underlying the upregulation of LOXL1 in both clinical specimens and ICC cell lines, we
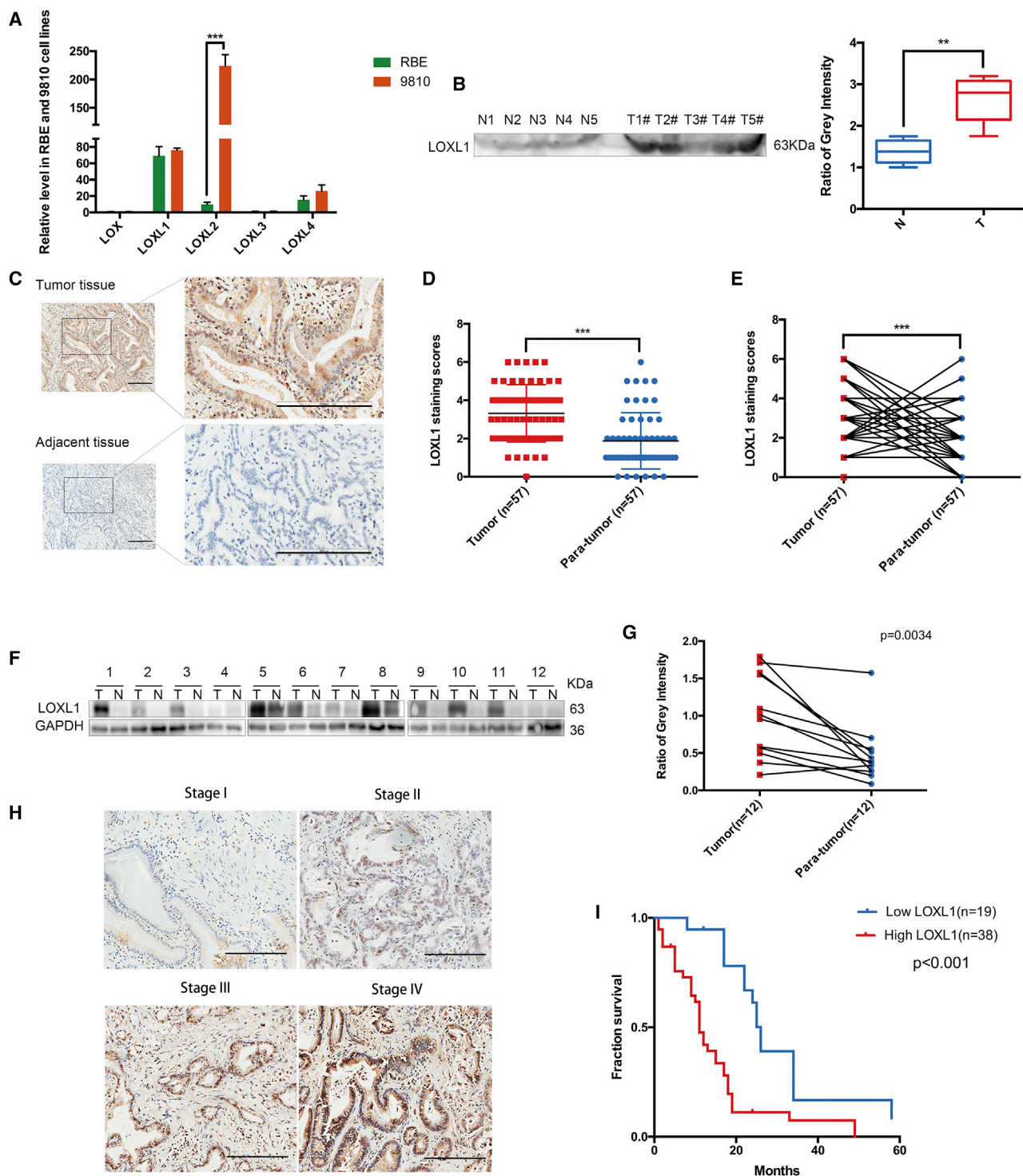
Figure 1. LOXL1 is upregulated in ICC and correlated with ICC progression and poor prognosis of ICC patients

(A) LOXL1 is overexpressed in both 9810 and RBE cell lines compared with other members of the LOX family. (B) LOXL1 protein is at a low level in blood serum samples of normal people (N) compared to blood serum samples of ICC patients (T). (C–E) The relative expression of LOXL1 protein in 57 paired ICC tumor tissues and adjacent normal tissues. Scale bars, 200 μm (***p < 0.001, paired Student's t test and Mann-Whitney U test). (F and G) Expression levels of LOXL1 in primary ICC tissues (T) and their paired nontumor tissues (N) were evaluated by western blotting. (H) Representative IHC staining images of ICC patients in different clinical stages (*AJCC Cancer Staging Manual 8th Edition*, stages I, II, III, and IV). (I) Kaplan-Meier curve of ICC patients' overall survival based on LOXL1 expression. Low LOXL1, n = 19; high LOXL1, n = 38 (*p < 0.05, **p < 0.01, ***p < 0.001).

constructed a lentivirus overexpression vector of LOXL1 (LV-OE-LOXL1). Lentivirus-mediated overexpression of LOXL1 in RBE and 9810 cells resulted in the generation of the stable ICC$_{LV-OE-LOXL1}$ cell line, which can highly express LOXL1 *in vivo*. The overexpression efficiency of LOXL1 was assessed by qRT-PCR and western blotting (Figures 3A and 3B). The proliferation and migration phenotypes were also tested in the ICC$_{LV-OE-LOXL1}$ cells, again confirming the function of LOXL1 in ICC. The proliferation ability was significantly enhanced in the stable ICC$_{LV-OE-LOXL1}$ cells in the CCK8 assays (Figure 3C). Moreover, more cell clones were generated in the colony-formation assay upon the stable overexpression of the LOXL1 protein in these tumor cells (Figure 3D). Consecutively, Transwell assays revealed that overexpression of LOXL1 in 9810 and RBE cells promoted their ability to move across the chamber membrane (Figure 3E). We further tested pAKT and pErk1/2 by western blotting, and as expected, the protein levels of pAKT and pErk1/2 were distinctly higher in stable ICC cell lines than in the NC groups (Figure 3F).

EMT has been shown to have an impact on the changes of cell phenotypes during the tumorigenic process, which depends on EMT-activating transcription factors (EMT-TFs) to participate in all stages of cancer progression.[15,16] However, the precise molecular and biochemical mechanisms underlying the induction of EMT-TFs are still poorly understood. To determine whether ICC undergoes the EMT process, we performed western blotting to examine the protein levels of EMT markers, such as E-cadherin, N-cadherin, and vimentin in tumor cells. E-cadherin was downregulated, whereas both N-cadherin and vimentin were upregulated in the LOXL1 overexpression group (Figure 3G).

Next, to study the expansion and migration ability of ICC cells overexpressing LOXL1 *in vivo*, stable RBE$_{LV-OE-LOXL1}$ and scramble RBE cells were implanted into immunodeficient nude mice. The subcutaneous tumor size was measured weekly until the mice were euthanized after 5 weeks. Tumors derived from the stable RBE$_{LV-OE-LOXL1}$ cells grew more rapidly than those from the scramble group. Moreover, compared with the control group, mice inoculated with stable RBE$_{LV-OE-LOXL1}$ cells had a larger average tumor volume after 5 weeks of inoculation (Figure 3H).

During the dissection of the mice, we observed that the density of vessels around subcutaneous tumors in the LOXL1 overexpression group was much higher than that in the scramble group (Figure 3H), which was further confirmed by IHC staining of CD31, CD34 (the markers of VECs),[17] and proliferating cell nuclear antigen (PCNA). In general, the xenografts of the LOXL1 overexpression group displayed higher levels of CD31, CD34, and PCNA (Figure 3I).

ICC is usually located inside the liver, adjacent to the bodies' arteries, veins, and lymph vessels. The involvement of vascular structures and lymph nodes is common in ICC. To determine whether secreted LOXL1 could stimulate angiogenesis by directly activating VECs, we collected the supernatant of stable ICC$_{LV-OE-LOXL1}$ and scramble ICC cells. The abundance of secreted LOXL1 was detected in the same vol-

**Table 1. Correlation of LOXL1 expression with the clinicopathological characteristics in ICC cases**

Characteristic	No. of cases	Positive (%)	Negative (%)	p value
Age				
<60	21	13 (61.9)	8 (38.1)	0.575
≥60	36	25 (69.4)	11 (30.6)	
Gender				
Male	32	20 (62.5)	12 (37.5)	0.574
Female	25	18 (72.0)	7 (28.0)	
TNM stage (AJCC)				
0−I	15	4 (26.7)	11 (73.3)	<0.001[a]
II−IV	42	34 (81.0)	8 (19.0)	
Microvascular invasion				
Present	39	32 (82.1)	7 (17.9)	0.001[a]
Absent	18	6 (33.3)	12 (66.7)	
Tumor differentiation				
Well or moderate	23	14 (60.9)	9 (39.1)	0.569
Poor	34	24 (70.6)	10 (29.4)	
Lymph node metastasis				
Present	40	34 (85.0)	6 (15.0)	<0.001[a]
Absent	17	4 (23.5)	13 (76.5)	
Liver metastasis				
Present	36	31 (86.1)	5 (13.9)	<0.001[a]
Absent	21	7 (33.3)	14 (66.7)	
Total	57	38 (66.7)	19 (33.3)	

The "LOXL1 expression" spanning header covers the Positive (%) and Negative (%) columns.

[a]p < 0.05.

ume of supernatant from two ICC cell lines. Then, human umbilical vein endothelial cells (HUVECs) treated with the supernatant containing the secreted LOXL1 were tested for their tube-formation ability. The supernatant of stable ICC$_{LV-OE-LOXL1}$ cells contained more LOXL1 protein than that of scramble ICC cells, as shown by western blotting results (Figure 3J). Briefly, HUVECs were cultured on a μ-Slide Angiogenesis plate (ibidi). Cells at the lower portion of the plate were injected with thawed Matrigel, and then supernatants of stable ICC$_{LV-OE-LOXL1}$ and scramble ICC cells were separately added to cells at the upper portion of the plate. After 2 h of incubation, we compared their proangiogenesis ability by counting the numbers of formed tubes and nodes. The stable transfection group showed a stronger ability to promote the formation of VEC tube-like structures than did the scramble group (Figure 3J). These results indicated that LOXL1 promoted ICC tumor growth and angiogenesis both *in vitro* and *in vivo* under the facilitation of EMT.

LOXL1 catalytic domain promoted angiogenesis of VECs by activating FAK and MAPK signaling pathways

To eliminate the interference of other proteins in the supernatant, we used purified LOXL1 protein in the tube-formation assays. LOXL1 was divided into five fragments, namely F1 (truncation of signal
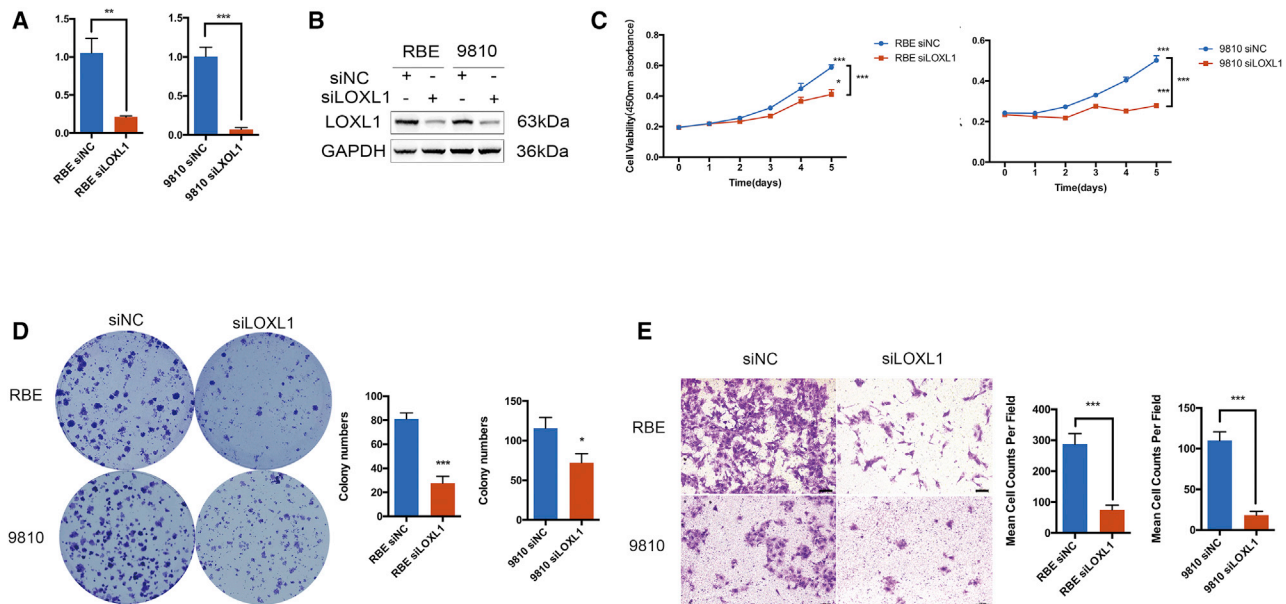
Figure 2. Silencing of LOXL1 weakens ICC cells' capacity for proliferation and metastasis

(A and B) Measure the knockdown efficiency of LOXL1 transfected by NC and siRNA through real-time PCR and western blot. (C) Effects of LOXL1 knockdown on proliferation of RBE and 9810 cells tested by CCK8 assays. (D) Knockdown of LOXL1 suppressed colony formation in RBE and 9810 cells. (E) Effects of LOXL1 knockdown on metastasis ability in RBE and 9810 cell lines. Scale bars, 100 μm. Error bars indicate the mean ± SE of three independent experiments (*p < 0.05, **p < 0.01, ***p < 0.001).

peptide, spanning residues 26−574 amino acids [aa]), F2 (truncation of both signal and pro-peptides, spanning residues 95−574 aa), F3 (middle fragment, residues 106−574 aa), F4 (catalytic domain [CD], residues 367−574 aa), and F0 (full-length protein) (Figures 4A and 4B). During the purification trials of these five protein fragments, only the F4 (LOXL1^{CD}) protein was proven to be stably expressed in the *E. coli* system. A glutathione S-transferase (GST)-fusion construct pGEX-6p-1-LOXL1^{CD} carrying a GST tag at the N terminus was generated. The recombinant protein was obtained through a GST purification system, as described in Materials and methods (Figures 4C and 4E). We further confirmed its reliability by human rhinovirus (HRV) 3C protease digestion and mass spectrum identification (Figures 4D and S2).

To verify the function of the LOXL1^{CD} protein, site-specific mutants were generated. According to the sequence alignment and structural comparison with LOXL2[18] (Figures S3−S5), key residues important for the catalytic activity were substituted with alanine. A double mutant was generated, of which H449 and H451 corresponding to H626 and H628 in LOXL2, respectively, were replaced with alanine. The proangiogenic abilities of GST, GST-LOXL1^{CD}, and GST-LOXL1^{CD} H449/H451A were detected through tube-formation assays (Figure 4F). Among these, only GST-LOXL1^{CD} could promote the formation of vessel-like structures by VECs, suggesting that the CD of LOXL1 is required for its proangiogenic function.

pFAK and the subsequent MAPK signaling pathway have been reported to be activated in VECs during the process of angiogenesis.[19]

To test whether GST-LOXL1^{CD} was able to activate FAK and the MAPK signaling pathway, lysates of cells treated with GST-LOXL1^{CD} and GST-LOXL1^{CD} H449/H451A were collected separately for measuring pFAK and pErk1/2 by western blotting. Compared with the double mutant, which disrupted the catalytic activity of LOXL1, the levels of FAK pY861 and pErk1/2 were upregulated by GST-LOXL1^{CD}, whereas the levels of FAK pY397 were not changed (Figure 4G). These findings indicated that GST-LOXL1^{CD} promotes the angiogenesis of HUVECs *in vitro* by regulating the FAK and MAPK signaling pathways.

LOXL1 directly interacted with FBLN5 both inside and outside cells

To further elaborate the molecular mechanism underlying the proangiogenic function mediated by LOXL1, we retrieved related data on potential proteins that might be critical for LOXL1 function. FBLN5 achieved the highest score among the predicted candidates in the Database: String (Figures 5A and S6). FBLN5 is a 55-kDa glycoprotein, also known as a developmental arteries and neural crest EGF-like (DANCE) protein. It is a matricellular protein containing a consensus RGD motif (Figure 5A), which mediates the binding of a subset of integrins, including α5β1, αvβ3, and αvβ5.[20] Schluterman et al.[21] reported that FBLN5 reduced fibronectin-mediated, integrin-induced reactive oxygen species (ROS) production by competing with fibronectin for binding to the α5β1 integrin. The formation of elastin fiber is an essential function of FBLN5.[22] Tang et al.[23] found that FBLN5 could affect the adhesion, migration, and invasion of hepatocellular carcinoma cells via an integrin-dependent mechanism.
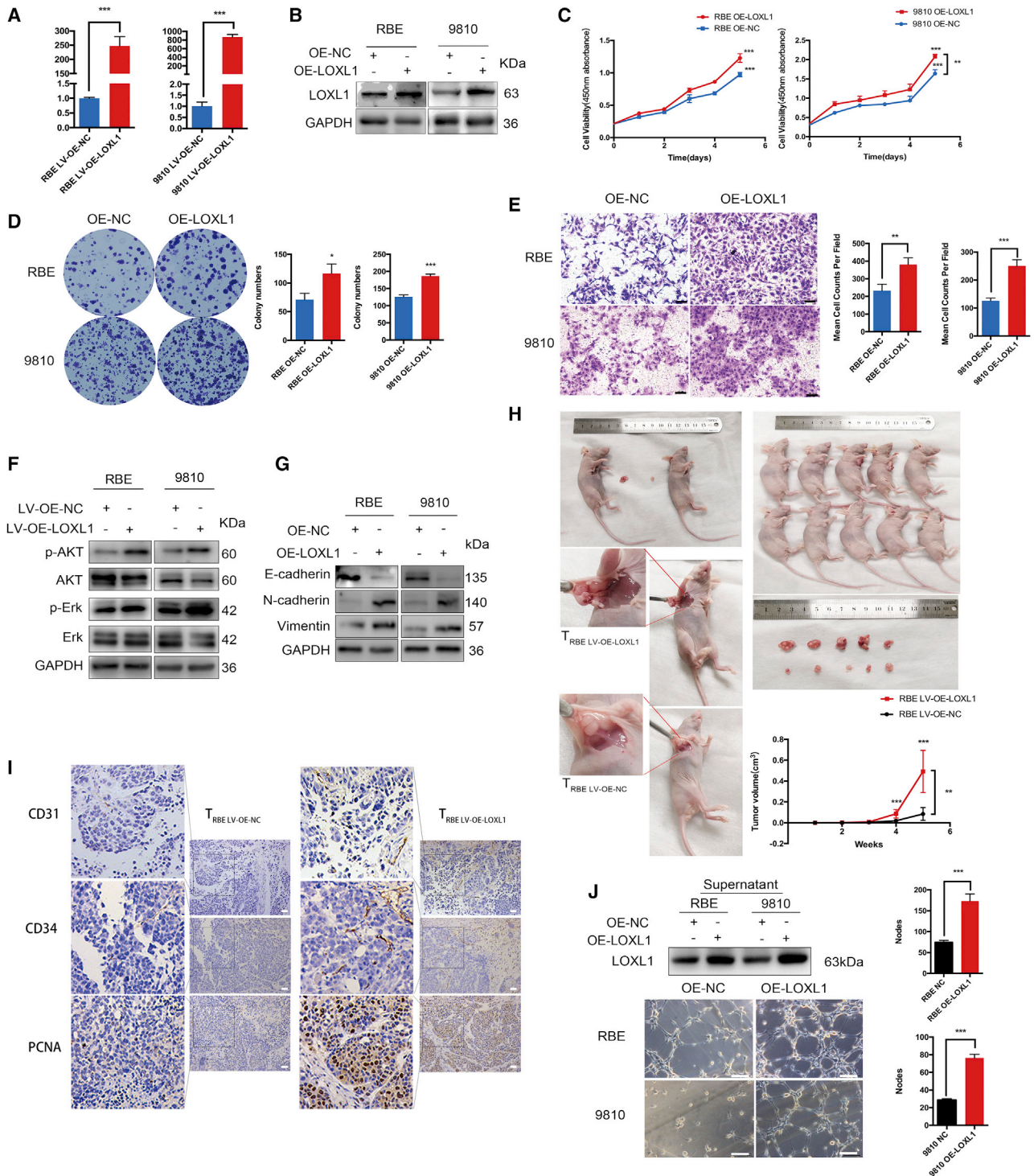
Figure 3. LOXL1 promotes ICC cell growth, metastasis, and angiogenesis

(A and B) Lentivirus-mediated LOXL1 overexpression in RBE and 9810 cells. (C) Cell proliferation was enhanced in LOXL1-overexpressed RBE and 9810 cells. (D) Over-expression of LOXL1 promoted colony formation of RBE and 9810 cells. (E) Transwell assays were performed in LOXL1-overexpressed RBE and 9810 cells. (F) The levels of phosphorylated (p)AKT, total AKT, pErk, and total Erk were measured in NC and LOXL1-overexpressed cells by western blot. (G) Western blot analysis of EMT-related proteins: E-cadherin, N-cadherin, and vimentin. (H) Images of xenografts in nude mice injected separately with LV-OE-NC and LV-OE-LOXL1 RBE cells. Tumor sizes were

(legend continued on next page)

To validate the interaction between FBLN5 and LOXL1, we transfected ICC cells with a Flag-tagged LOXL1 overexpression lentivirus and performed an exogenous coIP assay in these cells. FBLN5 could be coimmunoprecipitated by Flag-tagged LOXL1 both inside and outside ICC cells (Figures 5B and 5C). Endogenous reciprocal coIP in a concentrated supernatant confirmed the interaction between FBLN5 and LOXL1 (Figure 5D). In addition, LOXL1 and FBLN5 were observed to be colocalized in ICC tissues by immunofluorescence (Figure 5E). All of these data indicated that LOXL1 could directly interact with FBLN5 both inside and outside cells.

FBLN5 RGD motif was essential for the proangiogenesis function of LOXL1 in ICC through binding to the αvβ3 integrin

The evolutionarily conserved RGD motif,[20] which is the most common ligand recognition site of integrins, is located at the N terminus of FBLN5. The RGD sequence exists not only in FBLN5 but also in many other matricellular and ECM proteins, such as fibronectin, vitronectin, and thrombospondins.[24] To explore whether the RGD motif exerts an important function in the LOXL1-induced proangiogenesis process of ICC, a mutant RGD sequence with alteration of the third amino acid from aspartate (D) to glutamate (E) was generated, thus retaining the fundamental function of FBLN5 yet abrogating its integrin-binding ability.[10,25] Moreover, as the αvβ3 integrin was reported to be the key integrin in RGD-dependent angiogenesis, cyclo (-RGD-d-phenylalanine-lysine [RGDfK]), a specialized inhibitor of the αvβ3 integrin, was applied as a variable in this experiment.

The transfection efficiency of RBE cells with the FBLN5^{RGD} (pFBLN5^{RGD}) and FBLN5$^{arginine-glycine-glutamate (RGE)}$ (pFBLN5^{RGE}) plasmids was tested by western blotting before the measurement of the secreted FBLN5 levels in the supernatant of the three treated groups (Figure 6A). Subsequently, the tube-formation assays were conducted under different conditions, confirming the interrelations among the RGD motif, αvβ3 integrin, and LOXL1 (Figure 6B). With the consideration of the efficiency of HUVECs for tube formation, we performed these *in vitro* assays by treating HUVECs with 100 ng/μL GST-LOXL1^{CD} protein to simulate the secreted LOXL1 produced *in vivo*. As expected, pFBLN5^{RGD} was shown to promote tube formation by HUVECs induced by GST-LOXL1^{CD} compared with the pFBLN5^{RGE} and pUC57 groups. Besides, application of the αvβ3 integrin inhibitor eliminated the effects of pFBLN5^{RGD} on the ability of HUVECs to form tubes. The inhibitory effects were apparent in the pUC57 group (Figures 6B and 6C). Moreover, compared with that in the pUC57 group, pFAK pY861 and pErk1/2 were upregulated in the pFBLN5^{RGD} group and downregulated in the pFBLN5^{RGE} group (Figure 6D), consistent with the trend of cell phenotypes. pFAK and pErk1/2 were dramatically downregulated upon treatment of HUVECs with cyclo (-RGDfK). Both pFBLN5^{RGD} and pFBLN5^{RGE} were able to reverse these phosphorylation effects, whereas pFBLN5^{RGD} exhibited a stronger rescue effect.

To examine the interactions among LOXL1, FBLN5, and the αvβ3 integrin more intuitively, a triple immunofluorescence colocalization assay was performed in ICC tumor tissues. LOXL1, FBLN5, and the αvβ3 integrin colocalized with each other along the vessel-like structures (Figure 6E), suggesting that LOXL1, FBLN5, and the αvβ3 integrin may form a complex *in vivo*. Collectively, the binding of LOXL1 to FBLN5 and the αvβ3 integrin on the surface of VECs was indispensable for the proangiogenic function of LOXL1 in activating the FAK and MAPK signaling pathways in VECs.

DISCUSSION

Both ICC and gallbladder cancer (GBC) are extremely malignant tumors of digestive organs, and although huge progress was recently made regarding the molecular biological behavior of GBC,[26–28] the mechanism underlying tumor formation and progression in ICC has not been fully elucidated. Many cases of ICC are diagnosed incidentally, and there are only a few effective therapeutic targets, with surgical resection being the main curative strategy for ICC. In this study, we tried to identify a protein biomarker that would facilitate the distinction of patients with ICC from unaffected people and serve as a potential therapeutic target with an indispensable role in the process of ICC, so as to develop alternative treatments for patients with ICC.

Previous studies showed that LOXL1 plays different roles in different tumors. LOXL1 is downregulated in bladder cancer cells, and this downregulation is mainly related to epigenetic mechanisms. LOXL1 acts as a tumor-suppressor gene in bladder cancer by inhibiting colony formation and antagonizing Ras activation of the ERK signaling pathway.[8] In contrast, LOXL1 is upregulated and acts as an oncogene in non-small cell lung cancer,[29] glioma,[30] colorectal cancer,[31] and prostate cancer.[32] Here, we found that the levels of LOXL1 were elevated in both the tumor tissues and blood serum of patients with ICC, with patients exhibiting a lower expression level having improved prognosis. The results of our clinicopathologic analysis indicated the positive correlation of LOXL1 with the tumor size, lymph nodes affected, metastases (TNM) stage (8th American Joint Committee on Cancer [AJCC]-TNM classification of malignant tumors), microvascular invasion, lymph node, and liver metastasis. We supposed that LOXL1 acted as a tumor promoter in ICC. In particular, LOXL1 was revealed to promote the proliferation of ICC by improving pAKT and pErk1/2 proteins, which are critical mediators in the MAPK and phosphatidylinositol 3-kinase (PI3K) signaling pathways. In addition, the ability to metastasize was also elevated in ICC cells through EMT. These results were consistent with some previous studies suggesting that LOXL1 might play a pivotal role in various tumors, including non-small cell lung,[29] gastric,[33] and human bladder[8] cancers.

Vascular invasion was once reported to be correlated with a poor prognosis in patients with ICC.[34] Research on ICC *in vitro* and *in vivo*

---

calculated every week, and statistical results came from five independent samples. (I) The expression of CD31, CD34, and PCNA was detected in ICC xenografts by IHC. (J) Secreted LOXL1 level in the supernatant of ICC cells could be improved by lentivirus-mediated LOXL1 overexpressed in RBE and 9810 cells and stimulated angiogenesis of VECs in vitro. Scale bars, 100 μm (*p < 0.05, **p < 0.01, ***p < 0.001).
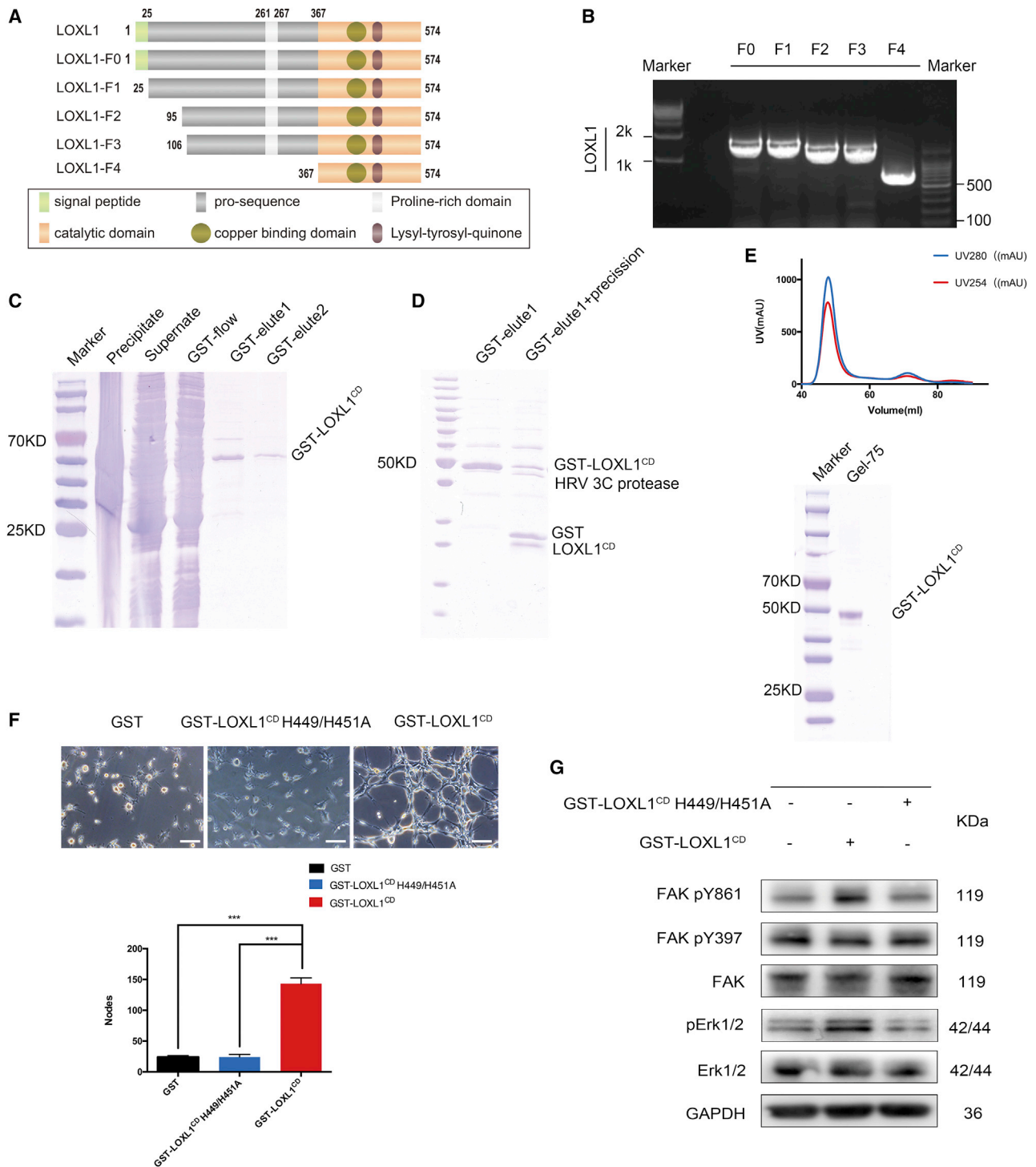
Figure 4. LOXL1^{catalytic domain (CD)} promotes angiogenesis of VECs by activating the FAK and MAPK signaling pathway

(A) Schematic illustration of LOXL1 structure: LOXL1 full-length was divided into five fragments for further purification: F0 (full-length protein), F1 (truncation of signal peptide, spanning residues 26−574 aa), F2 (truncation of both signal and pro-peptides, spanning residues 95−574 aa), F3 (middle fragment, residues 106−574 aa), and F4 (CD, residues 367−574 aa). (B) DNA electrophoresis of five fragments. (C) Purification of GST-LOXL1^{CD} by passing through a GST column. (D) Identification of GST-LOXL1^{CD} by HRV 3C protease digestion. (E) Purification of GST-LOXL1^{CD} by passing through a size-exclusion chromatography column. (F) GST-LOXL1^{CD} (wild-type [WT]) promoted angiogenesis of VECs compared to GST and GST-LOXL1^{CD} H449/H451A (mutant). Scale bars, 100 μm (*p < 0.05, **p < 0.01, ***p < 0.001). (G) pFAK pY861 and pErk1/2 in VECs was upregulated by GST-LOXL1^{CD}.

showed that the density of blood vessels was correlated with the protein level of LOXL1, which further suggested that the procarcinogenesis function of LOXL1 in ICC might involve angiogenesis as a crucial intermediate step.

As one prototypical member of the LOX family, the documented function of LOXL1 is to catalyze peptidyl lysine substrates to highly reactive aldehydes, especially during the covalent crosslinking process of collagens and elastin.[18,35] Moreover, LOXL1 has been shown to perform various intracellular functions in tumors, whereas the secreted LOXL1 might have more impacts on tumor progression by affecting the tensile strength and structural reconstruction of tumor tissues.[7] To figure out the proangiogenic function of the secreted LOXL1, we purified LOXL1^{CD}, the active domain of LOXL1, and found that LOXL1^{CD} promoted the angiogenesis of VECs compared with its mutant counterpart by upregulating pFAK pY861 and pErk1/2.

It is widely known that integrins on the surfaces of VECs can regulate the process of angiogenesis,[36,37] which is usually mediated by the combination of the RGD motif and integrins.[38,39] The RGD motif is known to exist in various stromal cells and ECM proteins, including fibronectin, vitronectin, and thrombospondin. The RGD motif has been reported to be recognized by integrin receptors and participates in many cell functions.[40,41] With the use of the protein-interaction prediction in the String database, we identified FBLN5 containing an RGD domain as the candidate with a high probability of interacting with the LOXL1 protein. This interaction was confirmed to exist both inside and outside ICC cells through coIP assays using ICC cells and supernatant samples, as well as through immunofluorescence assays using ICC tissues. Previous studies showed that full exposure of the RGD sequence and the presence of FBLN5 flanking sequences were necessary for the binding of FBLN5 to integrins.[42] We speculated that the secreted LOXL1 protein bound to the FBLN5 protein with its exposed RGD domain, and then the resulting complex bound to αvβ3 on the surface of VECs, thereby regulating the FAK and MAPK signaling pathways in VECs and promoting angiogenesis. By mutating the RGD sequence and using an inhibitor of αvβ3, we identified that the RGD domain in FBLN5 and αvβ3 was indispensable for the proangiogenic function of LOXL1. In addition, triple immunofluorescence tests in ICC tissues intuitively showed the colocalization of LOXL1, FBLN5, and αvβ3.

In summary, we found that upregulation of LOXL1 promoted the proliferation of ICC cells by improving pAKT and pErk and facilitating the migration ability of ICC cells through EMT, proposing a model of the intracellular function of LOXL1 in ICC. Regarding the function of LOXL1, we demonstrated that secreted LOXL1 interacted with FBLN5 to expose its RGD domain and stimulated angiogenesis by regulating the FAK and MAPK signaling pathways in VECs through binding to the αvβ3 integrin. These findings provide novel strategies for selecting therapeutic molecular targets for ICC treatment, especially in patients with advanced ICC. Particularly, LOXL1 can serve as a potential therapeutic target for the clinical therapy of ICC.

MATERIALS AND METHODS

Serum, specimens, and patients
The serum of five normal people and five ICC patients and twelve pairs of tumor and adjacent tissue samples were obtained from healthy adults in the Shanghai Key Laboratory of Biliary Tract Disease Research and individuals diagnosed with ICC who were confirmed by pathological diagnosis after surgical resection in the Xinhua Hospital Affiliated to Shanghai Jiaotong University School of Medicine from 2013 to 2019. Clinicopathological data and paired tissue specimens were from 57 ICC patients from 2010 to 2015 at the Department of General Surgery in Xinhua Hospital. All ICC patients above underwent radical cholecystectomy without taking any prior radiotherapy or chemotherapy treatments, and tissue samples for immunoblotting analysis were cryopreserved in liquid nitrogen immediately until use. Participants enrolled in this study provided consent for the use of serum and tumor tissues. Our study was approved by the Ethics Review Committee of Xinhua Hospital.

RNA extraction and qRT-PCR
RNA extraction of cells or tissues was carried out according to the manufacturer's instructions by using TRIzol (Takara, Shiga, Japan). Standard RT-PCR amplification was performed under the control of the StepOnePlus system by using SYBR Master Mix (Takara, Shiga, Japan), and (GAPDH) was used as an endogenous control. The primers used are listed in Tables S1–S3.

Cell culture
ICC cell lines (RBE and 9810) and HUVECs were purchased from Cell Bank of the Shanghai Institute for Biological Sciences, Chinese Academy of Sciences (Shanghai, China), and verified by short tandem repeat (STR) analysis (Figure S8). RBE cells and HUVECs were cultured in Dulbecco's modified Eagle's medium (DMEM; Gibco, USA), blended with 10% fetal bovine serum (FBS), 10 U/mL penicillin, and 0.1 mg/mL streptomycin (complete medium). 9810 cells were cultured in complete RPMI-1640 medium (HyClone, Logan, TX, USA).

Concentration of supernatant and secreted protein preparation
After filtration with the use of 0.25 μm filters, the supernatant was collected into Amicon Ultra-15 Centrifugal Filter Units (UFC900324; Millipore) and concentrated at 4,000 rpm for 30 min to 90 min to reach the desired volume for further use.

IHC analysis of tissues
The paraffin-embedded sections were prepared first. Anti-human-LOXL1 antibody (Abcam), anti-PCNA (Cell Signaling Technology), anti-CD31 (ABclonal), and anti-CD34 (ABclonal) were separately used as the primary antibodies, followed by goat anti-rabbit immunoglobulin G (IgG) antibody incubation. The slides were counterstained with ChemMate hematoxylin (DakoCytomation, Kyoto, Japan) and mounted. Two independent investigators who were blind to the cases were invited to observe these slides under a microscope (Leica,
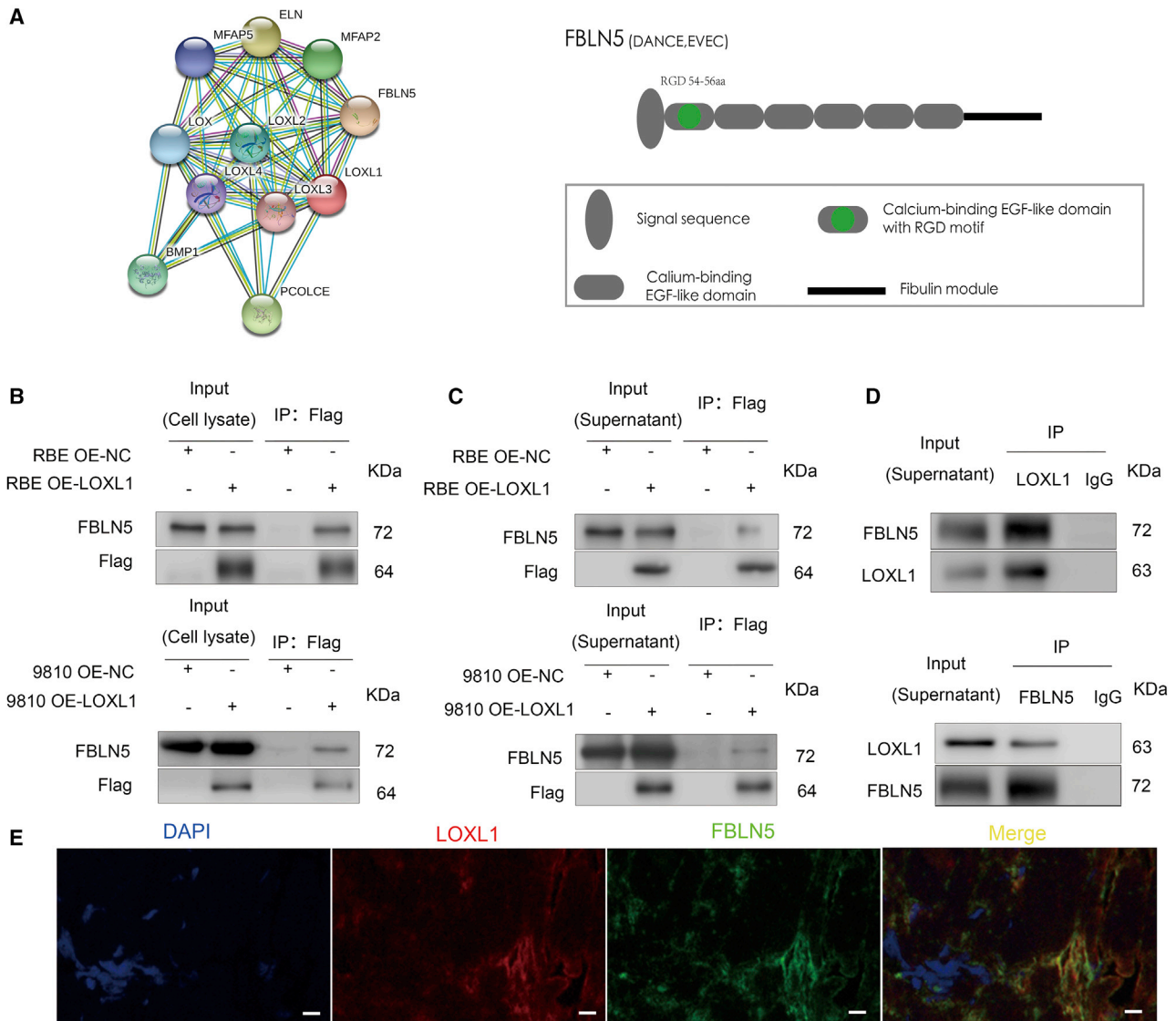
Figure 5. LOXL1 directly interacts with FBLN5

(A) Predicted protein-protein interaction network and structure diagram of FBLN5 sequence. (B) LOXL1 physically interacts with FBLN5 inside ICC cells. The exogenous proteins in the NC group (RBE OE-NC) and lentivirus-mediated LOXL1 overexpression group (RBE OE-LOXL1) were immunoprecipitated with the Flag antibody followed by a western blot test and 10% lysis for input. (C) LOXL1 interacts with FBLN5 outside ICC cells. The secreted proteins in the supernatant of RBE OE-NC and RBE OE-LOXL1 were immunoprecipitated with the Flag antibody, followed by a western blot test and 10% lysis for input. (D) The secreted proteins of endogenous LOXL1 and FBLN5 were immunoprecipitated with IgG and antibodies against LOXL1 and FBLN5 in the supernatant of RBE cells, followed by a western blot test and 10% lysis for input. (E) Co-localization of LOXL1 and FBLN5 in the extracellular matrix of ICC tumor tissues. Scale bars, 100 μm.

Wetzlar, Germany) and analyze the results following semiquantitative rules.[43]

Immunofluorescence of tumor tissues

Double and triple immunofluorescent staining of tumor tissues was carried out, referring to the instructions. Briefly, the slides of tissues were prepared through deparaffinization and a quenching procedure of endogenous peroxidase, and the slides were incubated with primary antibodies against LOXL1 (Abcam), FBLN5 (ABclonal), or the αvβ3 integrin (Abcam), overnight at 4°C. After washed three times with phosphate-buffered saline (PBS) and blocked with goat serum, the slides were incubated with different fluorescein-labeled secondary antibodies. Slides were viewed and photographed with a confocal microscope (Leica).

Reagents, plasmids, and lentivirus infection

siRNA was synthesized by GenePharma (Shanghai, China). The sequences of siRNAs are listed in the Supplemental Information.
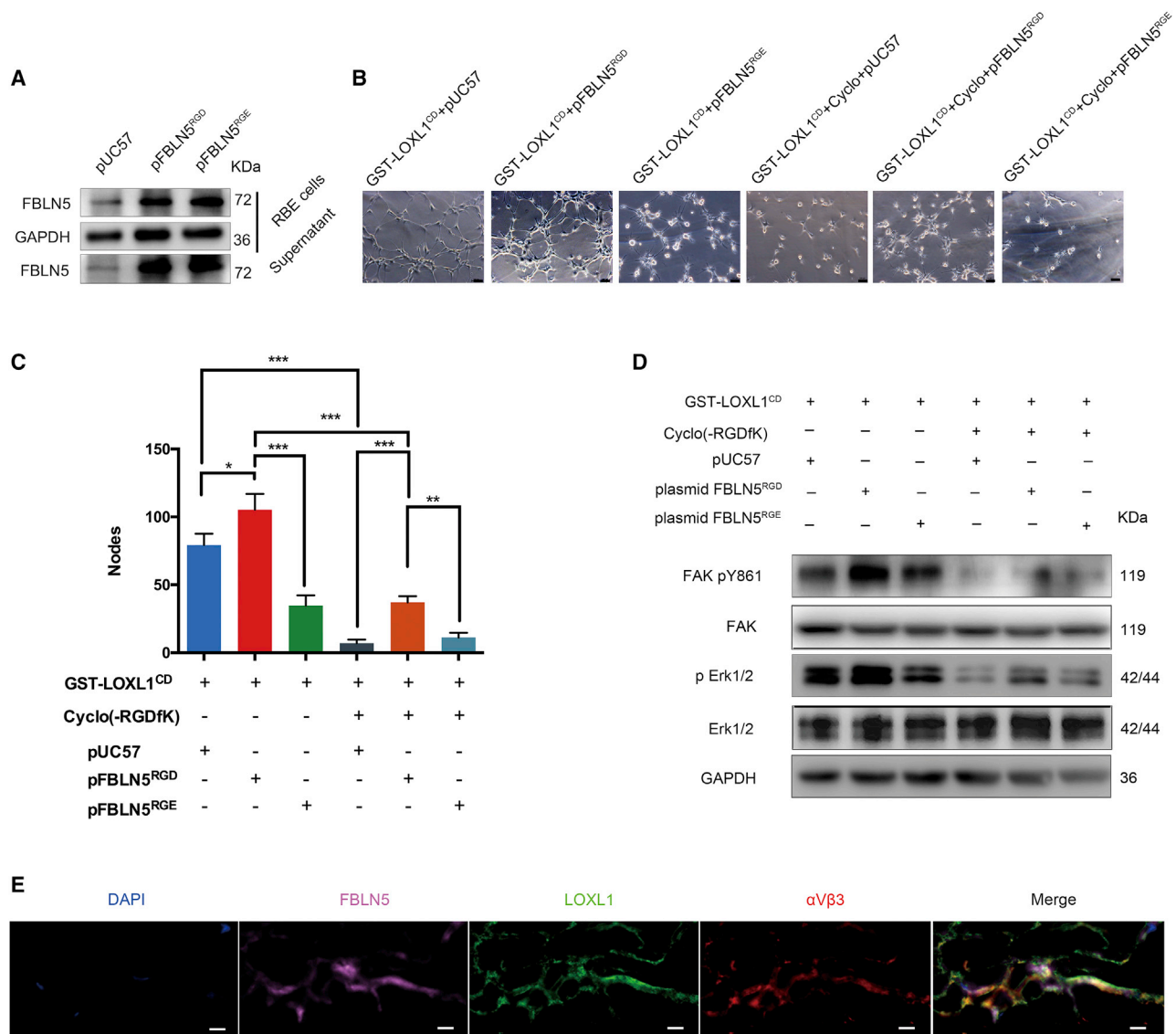
Figure 6. RGD domain in FBLN5 is indispensable to the proangiogenic function of LOXL1 in ICC by binding to the αvβ3 integrin

(A) pUC57, pFBLN5^{RGD}, and pFBLN5^{RGE} were transfected into RBE cells, and the efficiency of transfection was measured by western blot. A higher level of FBLN5 protein was contained in the supernatant of pFBLN5 transfected groups compared to pUC57 groups. (B and C) The roles of RGD domain and the αvβ3 integrin in the proangiogenic process of GST-LOXL1^{CD} were detected through tube-formation assays. Cyclo (-RGDfK) (50 ng/μL) was used to block the αvβ3 integrin. Scale bars, 100 μm (*p < 0.05, **p < 0.01, ***p < 0.001). (D) Cell lysates of VECs were collected for testing phosphorylation levels of FAK and Erk1/2 by western blot. (E) Colocalization of LOXL1, FBLN5, and the αvβ3 integrin along with the vessel-like structure in the extracellular matrix of ICC tumor tissues. Scale bars, 100 μm.

Lipofectamine 2000 Reagent (Life Technologies, USA) was used for siRNA transfection according to the instructions. The inhibitor of the αvβ3 integrin, cyclo (-RGDfK), was purchased from MedChemExpress (MCE; USA) and diluted to 50 μg/μL for stock. Plasmids of pUC57, pFBLN5^{RGD}, and pFBLN5^{RGE} were synthesized by GenScript (Nanjing, China) (Figure S7). The full length of LOXL1 was cloned to the lentivirus vector Ubi-MCS-3FLAG-CBh-gcGFP-IRES-puromycin. Recombinant lentivirus of the LV-OE-LOXL1 vector and empty vector of LV-OE-NC were synthesized by GeneChem

(Shanghai, China). Concentrated viruses were incubated with RBE and 9810 cells, and the transfected cells were cultured with puromycin following screening procedures of the instructions.

CCK8 cell proliferation assay, clone-formation assay, Transwell assay, and tube-formation assay

For proliferation assay, 1,000 RBE cells and the 9810 cells per well were seeded to 96-well plates after treatment. CCK8 (Dojindo Laboratories, Kumamoto, Japan) was used to assess cell numbers and

viability, and the absorbance was measured one time every day at 490 nm by using a spectrophotometric plate reader (BioTek, Saxony, Germany).

For clone-formation assay, the RBE and 9810 cells were seeded into 6-well plates (800 cells/well) after transfection and cultured in RPMI-1640 medium containing 10% FBS. After culturing at 37°C for 2 weeks, the colonies were fixed with paraformaldehyde for 15 min and then stained with crystal violet for 15 min.

For Transwell assay, fifteen thousand RBE cells and the 9810 cells in 200 μL serum-free culture medium were seeded into the top chamber. 600 μL medium with 20% FBS was added into the bottom chambers. The plates were incubated at 37°C for 18 h, and the cells on the downside surface of the semipermeable membrane were fixed and stained following the same protocols in the clone-formation assay.

For the tube-formation assay, endothelial cells were mixed with culture supernate, which is preconditioned with tumor cells, and then plated into ibidi chambers precovered with growth factor-reduced Matrigel at the density of 5×10^4 cells/well. Incubation of the ibidi plate was at 37°C and 5% CO_2 for 4−6 h.

Western blot analysis
Protein samples from tissues, cell lysates, or supernatants were lysed and denaturalized for analysis. The following procedures were performed as described previously:[27] anti-LOXL1, GAPDH, N-cadherin, E-cadherin, vimentin, AKT, pAKT, Erk, and pErk (Abcam, MA, USA). Flag-tag, FBLN5, FAK pY861, FAK pY397, and FAK (ABclonal, China) antibodies were used as primary antibodies to examine protein expressions. An ECL kit (Pierce; Thermo Fisher Scientific, Rockford, IL, USA) was used to detect specific signals.

Tumor xenograft models
All animal experiments were approved by the Ethics Committee of Xinhua Hospital Affiliated to Shanghai Jiaotong University School Of Medicine. BALB/c nude mice were first divided into two groups (OE-LOXL1 and OE-NC) and then injected subcutaneously with 4×10^6 RBE cells. Tumor growth was monitored and measured by using micrometer calipers weekly before the mice were killed. Tumor volumes were calculated as follows: tumor volume = width^2 (mm^2) × length (mm)/2. Tumors were harvested and stored in paraformaldehyde immediately for further IHC test.

Protein expression and purification
The CD of LOXL1 (residues 367−574 aa) was cloned into a pGEX-6p-1 vector between BamHI and SalI sites, which carry a GST tag at the N terminus. The sequences used here were shown as the following: LOXL1-367-pET28-BamHI forward (F): 5′-CGCGGATCCCGCGGT CTCCCTGACTTGGT-3′; LOXL1-574-pET28-SalI reverse (R): 5′-T GCGGCCGCAAGCTTGTCGACGCTATCAGGATTGGACAATTT TGCAGTTTG-3′. Recombinant proteins were expressed in *E. coli* strain BL21 (DE3) Gold (Agilent, USA). Cultures were grown in Luria-Bertani (LB) media at 37°C to an optical density 600 (OD$_{600}$) of

0.6. After induction with 0.2 mM isopropyl β-d-1-thiogalactopyranoside (IPTG), the cells were grown at 18°C for 16 h. The cells were harvested by centrifugation at 4°C and disrupted by French press (JNBio) in buffer S (20 mM Tris-HCl, pH 8.0, 500 mM NaCl, 1 mM EDTA, 0.1% 2-mercaptoethanol, and 1 mM PMSF) for GST-tag proteins. Bacterial lysates were clarified by centrifugation at 16,000 × g for 1 h. For recombinant GST-tag proteins, the supernatant was loaded onto a GSTrap HP column (GE Healthcare). After extensive washing with buffer S, the target protein was eluted by buffer S, supplemented with 10 mM glutathione-reduced form (GSH). Target proteins were further purified by passage through a HiLoad 16/60 Superdex 200 column (GE Healthcare) with buffer GF (10 mM Tris-HCl, pH 8.0, 500 mM NaCl, and 1 mM DTT). Fractions containing target proteins were pooled and concentrated for further use.

CoIP of LOXL1 and FBLN5
CoIP assays were performed under both endogenous and exogenous conditions. RBE and 9810 cells were transfected with lentivirus previously. Cells are incubated with NETN lysis buffer (20 mM Tris-HCl, pH 7.4, 150 mM NaCl, 0.5% NP40, 1 mM PMSF) for 30 min at 4°C. What's more, the supernatant of ICC cells was collected and concentrated by using Amicon Ultra-15 Centrifugal Filter Devices. Cell lysates or concentrated supernatant were incubated with anti-Flag magnetic bead antibodies (for exogenous detection) or pretreated with protein G beads and then immunoprecipitated with rabbit anti-LOXL1 and anti-FBLN5 antibody (for endogenous detection) overnight at 4°C, and anti-rabbit IgG was used to eliminate endogenous interference. The interaction results were analyzed by western blotting.

Statistical analysis
Clinicopathological features of ICC patients with LOXL1 expression were analyzed through the χ^2 test or Fisher's exact probability test. Kaplan-Meier plots and log-rank tests were used in survival analysis. The Student's t test was used to evaluate the differences between mean values, and the result was reported as the mean ± SD. Each experiment was repeated three times, and p < 0.05 was considered statistically significant. Statistical analysis was performed using SPSS statistical software.

SUPPLEMENTAL INFORMATION
Supplemental Information can be found online at https://doi.org/10.1016/j.omtn.2021.01.001.

AUTHOR CONTRIBUTIONS

DECLARATION OF INTERESTS

REFERENCES

1. Razumilava, N., and Gores, G.J. (2014). Cholangiocarcinoma. Lancet 383, 2168–2179.

2. Blechacz, B. (2017). Cholangiocarcinoma: Current knowledge and new developments. Gut Liver 11, 13–26.

3. Rizvi, S., and Gores, G.J. (2017). Emerging molecular therapeutic targets for cholangiocarcinoma. J. Hepatol. 67, 632–644.

4. Trackman, P.C. (2016). Lysyl oxidase isoforms and potential therapeutic opportunities for fibrosis and cancer. Expert Opin. Ther. Targets 20, 935–945.

5. Thomassin, L., Werneck, C.C., Broekelmann, T.J., Gleyzal, C., Hornstra, I.K., Mecham, R.P., and Sommer, P. (2005). The Pro-regions of lysyl oxidase and lysyl oxidase-like 1 are required for deposition onto elastic fibers. J. Biol. Chem. 280, 42848–42855.

6. Kagan, H.M., and Li, W. (2003). Lysyl oxidase: properties, specificity, and biological roles inside and outside of the cell. J. Cell. Biochem. 88, 660–672.

7. Barker, H.E., Cox, T.R., and Erler, J.T. (2012). The rationale for targeting the LOX family in cancer. Nat. Rev. Cancer 12, 540–552.

8. Wu, G., Guo, Z., Chang, X., Kim, M.S., Nagpal, J.K., Liu, J., Maki, J.M., Kivirikko, K.I., Ethier, S.P., Trink, B., and Sidransky, D. (2007). LOXL1 and LOXL4 are epigenetically silenced and can inhibit ras/extracellular signal-regulated kinase signaling pathway in human bladder cancer. Cancer Res. 67, 4123–4129.

9. Kowal, R.C., Richardson, J.A., Miano, J.M., and Olson, E.N. (1999). EVEC, a novel epidermal growth factor-like repeat-containing protein upregulated in embryonic and diseased adult vasculature. Circ. Res. 84, 1166–1176.

10. Nakamura, T., Ruiz-Lozano, P., Lindner, V., Yabe, D., Taniwaki, M., Furukawa, Y., Kobuke, K., Tashiro, K., Lu, Z., Andon, N.L., et al. (1999). DANCE, a novel secreted RGD protein expressed in developing, atherosclerotic, and balloon-injured arteries. J. Biol. Chem. 274, 22476–22483.

11. Sullivan, K.M., Bissonnette, R., Yanagisawa, H., Hussain, S.N., and Davis, E.C. (2007). Fibulin-5 functions as an endogenous angiogenesis inhibitor. Lab. Invest. 87, 818–827.

12. Yanagisawa, H., Davis, E.C., Starcher, B.C., Ouchi, T., Yanagisawa, M., Richardson, J.A., and Olson, E.N. (2002). Fibulin-5 is an elastin-binding protein essential for elastic fibre development in vivo. Nature 415, 168–171.

13. Hirai, M., Ohbayashi, T., Horiguchi, M., Okawa, K., Hagiwara, A., Chien, K.R., Kita, T., and Nakamura, T. (2007). Fibulin-5/DANCE has an elastogenic organizer activity that is abrogated by proteolytic cleavage in vivo. J. Cell Biol. 176, 1061–1071.

14. Nakamura, T., Lozano, P.R., Ikeda, Y., Iwanaga, Y., Hinek, A., Minamisawa, S., Cheng, C.F., Kobuke, K., Dalton, N., Takada, Y., et al. (2002). Fibulin-5/DANCE is essential for elastogenesis in vivo. Nature 415, 171–175.

15. Brabletz, T., Kalluri, R., Nieto, M.A., and Weinberg, R.A. (2018). EMT in cancer. Nat. Rev. Cancer 18, 128–134.

16. Nieto, M.A., Huang, R.Y.-J., Jackson, R.A., and Thiery, J.P. (2016). Emt: 2016. Cell 166, 21–45.

17. Shao, R., Hamel, K., Petersen, L., Cao, Q.J., Arenas, R.B., Bigelow, C., Bentley, B., and Yan, W. (2009). YKL-40, a secreted glycoprotein, promotes tumor angiogenesis. Oncogene 28, 4456–4468.

18. Zhang, X., Wang, Q., Wu, J., Wang, J., Shi, Y., and Liu, M. (2018). Crystal structure of human lysyl oxidase-like 2 (hLOXL2) in a precursor state. Proc. Natl. Acad. Sci. USA 115, 3828–3833.

19. Hood, J.D., Frausto, R., Kiosses, W.B., Schwartz, M.A., and Cheresh, D.A. (2003). Differential alphav integrin-mediated Ras-ERK signaling during two pathways of angiogenesis. J. Cell Biol. 162, 933–943.

20. Yanagisawa, H., Schluterman, M.K., and Brekken, R.A. (2009). Fibulin-5, an integrin-binding matricellular protein: its function in development and disease. J. Cell Commun. Signal. 3, 337–347.

21. Schluterman, M.K., Chapman, S.L., Korpanty, G., Ozumi, K., Fukai, T., Yanagisawa, H., and Brekken, R.A. (2010). Loss of fibulin-5 binding to beta1 integrins inhibits tumor growth by increasing the level of ROS. Dis. Model. Mech. 3, 333–342.

22. Zheng, Q., Davis, E.C., Richardson, J.A., Starcher, B.C., Li, T., Gerard, R.D., and Yanagisawa, H. (2007). Molecular analysis of fibulin-5 function during de novo synthesis of elastic fibers. Mol. Cell. Biol. 27, 1083–1095.

23. Tang, J.C., Liu, J.H., Liu, X.L., Liang, X., and Cai, X.J. (2015). Effect of fibulin-5 on adhesion, migration and invasion of hepatocellular carcinoma cells via an integrin-dependent mechanism. World J. Gastroenterol. 21, 11127–11140.

24. Bayless, K.J., Salazar, R., and Davis, G.E. (2000). RGD-dependent vacuolation and lumen formation observed during endothelial cell morphogenesis in three-dimensional fibrin matrices involves the $\alpha(v)\beta(3)$ and $\alpha(5)\beta(1)$ integrins. Am. J. Pathol. 156, 1673–1683.

25. Budatha, M., Roshanravan, S., Zheng, Q., Weislander, C., Chapman, S.L., Davis, E.C., Starcher, B., Word, R.A., and Yanagisawa, H. (2011). Extracellular matrix proteases contribute to progression of pelvic organ prolapse in mice and humans. J. Clin. Invest. 121, 2048–2059.

26. Li, M., Zhang, Z., Li, X., Ye, J., Wu, X., Tan, Z., Liu, C., Shen, B., Wang, X.A., Wu, W., et al. (2014). Whole-exome and targeted gene sequencing of gallbladder carcinoma identifies recurrent mutations in the ErbB pathway. Nat. Genet. 46, 872–876.

27. Shu, Y.-J., Weng, H., Ye, Y.-Y., Hu, Y.-P., Bao, R.-F., Cao, Y., Wang, X.-A., Zhang, F., Xiang, S.-S., Li, H.-F., et al. (2015). SPOCK1 as a potential cancer prognostic marker promotes the proliferation and metastasis of gallbladder cancer cells by activating the PI3K/AKT pathway. Mol. Cancer 14, 12.

28. Hu, Y.P., Jin, Y.P., Wu, X.S., Yang, Y., Li, Y.S., Li, H.F., Xiang, S.S., Song, X.L., Jiang, L., Zhang, Y.J., et al. (2019). LncRNA-HGBC stabilized by HuR promotes gallbladder cancer progression by regulating miR-502-3p/SET/AKT axis. Mol. Cancer 18, 167.

29. Zeltz, C., Pasko, E., Cox, T.R., Navab, R., and Tsao, M.-S. (2019). Loxl1 is regulated by integrin α11 and promotes non-small cell lung cancer tumorigenicity. Cancers (Basel) 11, 705.

30. Payne, S.L., Hendrix, M.J., and Kirschmann, D.A. (2007). Paradoxical roles for lysyl oxidases in cancer–a prospect. J. Cell. Biochem. 101, 1338–1354.

31. Hu, L., Wang, J., Wang, Y., Wu, L., Wu, C., Mao, B., Maruthi Prasad, E., Wang, Y., and Chin, Y.E. (2020). LOXL1 modulates the malignant progression of colorectal cancer by inhibiting the transcriptional activity of YAP. Cell Commun. Signal. 18, 148.

32. Nilsson, M., Adamo, H., Bergh, A., and Bergström, S.H. (2016). Inhibition of lysyl oxidase and lysyl oxidase-like enzymes has tumour-promoting and tumour-suppressing roles in experimental prostate cancer. Sci. Rep. 6, 19608.

33. Kasashima, H., Yashiro, M., Okuno, T., Miki, Y., Kitayama, K., Masuda, G., Kinoshita, H., Morisaki, T., Fukuoka, T., Hasegawa, T., et al. (2018). Significance of the lysyl oxidase members lysyl oxidase like 1, 3, and 4 in gastric cancer. Digestion 98, 238–248.

34. Jia, X., Lu, S., Zeng, Z., Liu, Q., Dong, Z., Chen, Y., Zhu, Z., Hong, Z., Zhang, T., Du, G., et al. (2020). Characterization of gut microbiota, bile acid metabolism, and cytokines in intrahepatic cholangiocarcinoma. Hepatology 71, 893–906.

35. Cox, T.R., Gartland, A., and Erler, J.T. (2016). Lysyl oxidase, a targetable secreted molecule involved in cancer metastasis. Cancer Res. 76, 188–192.

36. Desgrosellier, J.S., and Cheresh, D.A. (2010). Integrins in cancer: biological implications and therapeutic opportunities. Nat. Rev. Cancer 10, 9–22.

37. Humphries, J.D., Byron, A., and Humphries, M.J. (2006). Integrin ligands at a glance. J. Cell Sci. 119, 3901–3903.

38. Lechner, A.M., Assfalg-Machleidt, I., Zahler, S., Stoeckelhuber, M., Machleidt, W., Jochum, M., and Nägler, D.K. (2006). RGD-dependent binding of procathepsin X to integrin alphavbeta3 mediates cell-adhesive properties. J. Biol. Chem. 281, 39588–39597.

39. Longmate, W., and Dipersio, C.M. (2017). Beyond adhesion: emerging roles for integrins in control of the tumor microenvironment. F1000Res. 6, 1612.

40. Davis, G.E., Bayless, K.J., Davis, M.J., and Meininger, G.A. (2000). Regulation of tissue injury responses by the exposure of matricryptic sites within extracellular matrix molecules. Am. J. Pathol. 156, 1489–1498.

41. Ruoslahti, E., and Pierschbacher, M.D. (1987). New perspectives in cell adhesion: RGD and integrins. Science 238, 491–497.

42. Lomas, A.C., Mellody, K.T., Freeman, L.J., Bax, D.V., Shuttleworth, C.A., and Kielty, C.M. (2007). Fibulin-5 binds human smooth-muscle cells through alpha5beta1 and alpha4beta1 integrins, but does not support receptor activation. Biochem. J. 405, 417–428.

43. Xiang, S., Wang, Z., Ye, Y., Zhang, F., Li, H., Yang, Y., Miao, H., Liang, H., Zhang, Y., Jiang, L., et al. (2019). E2F1 and E2F7 differentially regulate KPNA2 to promote the development of gallbladder cancer. Oncogene 38, 1269–1281.